

## Polycyclic Aromatics with Flanking Thiophenes: Tuning Energy Level and Band Gap of Conjugated Polymers for Bulk Heterojunction Photovoltaics

Samuel C. Price, Andrew C. Stuart, and Wei You\*

Department of Chemistry, University of North Carolina at Chapel Hill, Chapel Hill, North Carolina 27599-3290

Received September 30, 2009; Revised Manuscript Received November 30, 2009

**ABSTRACT:** In the pursuit of donor–acceptor low band gap polymers for photovoltaic applications, finding an optimal donor monomer which maximizes the photovoltaic efficiency is a complex synthetic optimization problem. We synthesized three different bithiophenes flanking a center aromatic ring (pyrrole, benzene, or pyridine) as the donor monomers (**DTPr**, **DTBn**, and **DTPn**) with decreasing electron-donating ability. An array of six electrochemically and optically unique polymers were prepared by copolymerizing these three monomers with 2,1,3-benzothiadiazole and with thiophene. The optical, electronic, and photovoltaic properties of these polymers were investigated. Among this series, we found that the HOMO energy level of the polymer is dominated by the most electron-rich ring in the polymer backbone. The optical band gap, conversely, involves the entire polymeric system. Among the three donor monomers investigated, we identified that **DTBn**-based polymers exhibited the most potential in photovoltaic applications due to their moderately low band gaps and low HOMO energy levels.

### Introduction

As a cost-effective alternative to current mainstream silicon solar cells, polymeric solar cells, in particular, bulk heterojunction (BHJ) solar cells based on fullerene and its derivatives, have attracted extensive research attention and witnessed significant progress in recent years.<sup>1–4</sup> The record high efficiency has continually advanced to its current value of more than 6%<sup>5,6</sup> due to synergetic advancements in device optimization, the understanding of organic semiconductor physics, and new material development.

In PC<sub>61</sub>BM-based BHJ solar cells, the theoretical maximum  $V_{oc}$  of a device is determined by highest occupied molecular orbital (HOMO) energy level of the conjugated polymer, and the theoretical maximum  $J_{sc}$  of a device is largely dependent on the band gap of this conjugated polymer.<sup>1</sup> The most successful low band gap polymer design strategy to date for photovoltaic devices is the donor–acceptor alternating copolymer (or internal charge transfer copolymer) strategy, which has produced several polymers with photovoltaic power conversion efficiencies larger than 4.0%.<sup>5–14</sup> The HOMO level of these donor–acceptor copolymers is determined almost exclusively by the donor monomer.<sup>15,16</sup> In order to decrease the HOMO level (and raise the  $V_{oc}$  of the resulting photovoltaic cell), donors with “weaker” electron-donating ability should be applied to this strategy. However, while “weaker” donors will improve the  $V_{oc}$  by lowering the HOMO, they will also widen the band gap since the interaction between the electron-rich donor and the electron-poor acceptor is what lowers the band gap of these copolymers. Additionally, polymers with HOMO levels below  $-5.9$  eV exhibit higher rates of geminate charge recombination.<sup>17</sup> Thus, finding an optimal donor monomer which maximizes the photovoltaic efficiency is a complex synthetic optimization problem.

To systematically discover this optimal donor monomer, a design strategy based upon fusing aromatic rings of different oxidation potentials into bithiophene was envisioned. First, bithiophenes flanking a center aromatic ring was chosen as a

template, since fused thiophenes have produced several high mobility semicrystalline polymers, and the flanking thiophenes would reduce steric hindrance and create smaller dihedral angles with adjacent monomers. Then pyrrole, benzene, and pyridine were inserted into the bithiophene template to create three donor monomers of decreasing electron-donating ability. These three monomers were then copolymerized with 2,1,3-benzothiadiazole and with thiophene in order to study the optical, electronic, and photovoltaic properties of these polymers and to identify the most promising monomer for future study.

### Results and Discussion

**Monomer and Polymer Synthesis.** Two structural units, dithieno[3,2-*b*:2',3'-*d*]pyrrole (**DTPr**)<sup>18,19</sup> and benzo[1,2-*b*:4,5-*b'*]dithiophene (**DTBn**),<sup>20</sup> were synthesized according to literature procedures. Long branched alkyl chains were attached in the center pyrrole or benzene unit to ensure the solubility of resulting polymers. Both units were readily converted into distannylated monomers to copolymerize with dibrominated comonomers via Stille coupling polymerization, offering corresponding polymers (Scheme 1). The third structural unit, dithieno[3,2-*b*:2',3'-*e*]pyridine (**DTPn**), has also been reported in the literature.<sup>21</sup> However, in our efforts to synthesize dithienopyridines with long solubilizing alkyl chains, we encountered a great deal of difficulty with the established synthetic route.<sup>21</sup> The literature procedure employed a bromination (Scheme 1A) in the final steps of the synthesis, which offered the target molecules with very low yield when long alkyl chains were involved (6% when R = *n*-dodecyl).<sup>22</sup> With our particular substrates which possessed more bulky alkyl chains at the 8-position of the **DTPn**, the reported bromination procedure resulted in either inseparable mixtures or exceptionally low yields.

The distannyl intermediate of the literature bromination procedure could also serve as a polymerizable monomer for Stille coupling polymerization; however, metalation of **1** with *n*-BuLi according to the literature procedure resulted in a mixture of monostannyl and distannyl compounds

\*To whom all correspondence should be addressed. E-mail: wyou@email.unc.edu.

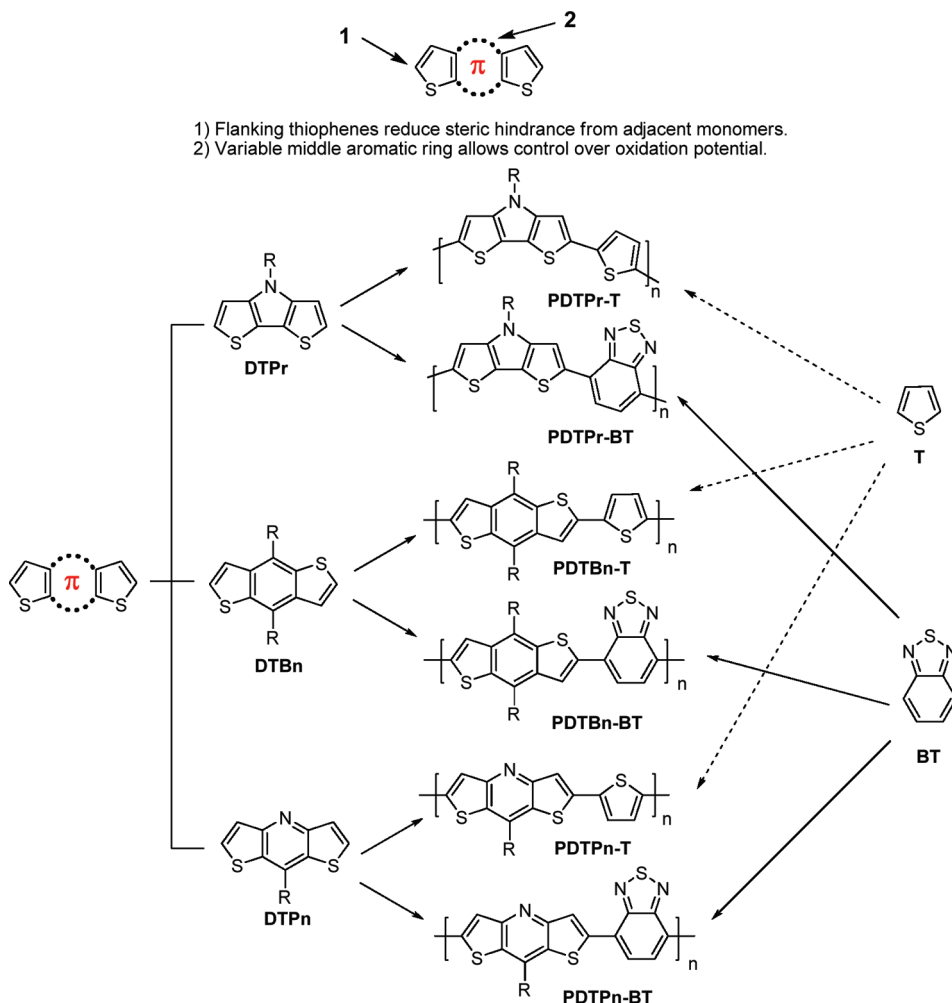
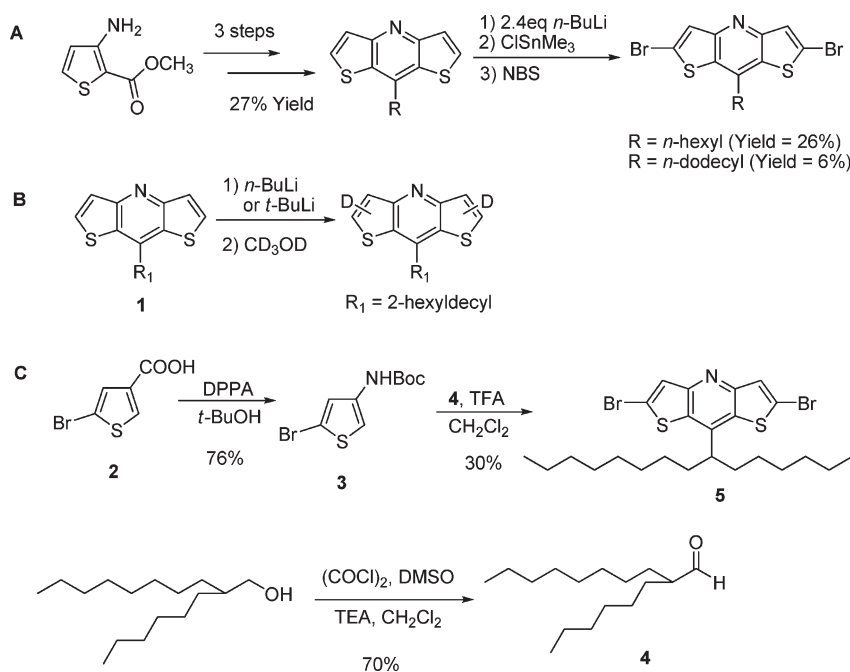


**Figure 1.** The library of structurally related polymers. “DT” stands for dithiophene. “Pr”, “Bn”, and “Pn” stand for fused pyrrole, benzene, and pyridine, respectively. “T” stands for thiophene and “BT” for benzothiadiazole.

**Scheme 1.** (A) Literature Procedure To Synthesize the Dibrominated DTPn; (B) Deuterium Labeling Experiment; and (C) Modified Synthetic Procedure of Dibrominated DTPn



which could not be separated. In an attempt to optimize the stannylation procedure, **1** was lithiated with *n*-BuLi and then quenched with deuterated methanol (Scheme 1B). This deuterium labeling experiment reveals that even after 5 h, the lithiation was not complete, and some starting material remained according to NMR (Figure 2). Attempts to opti-

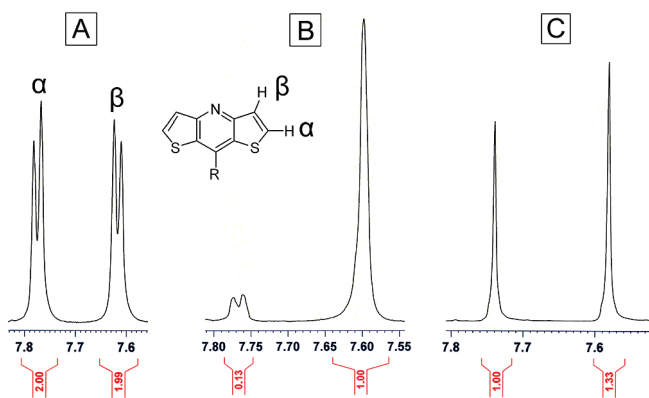
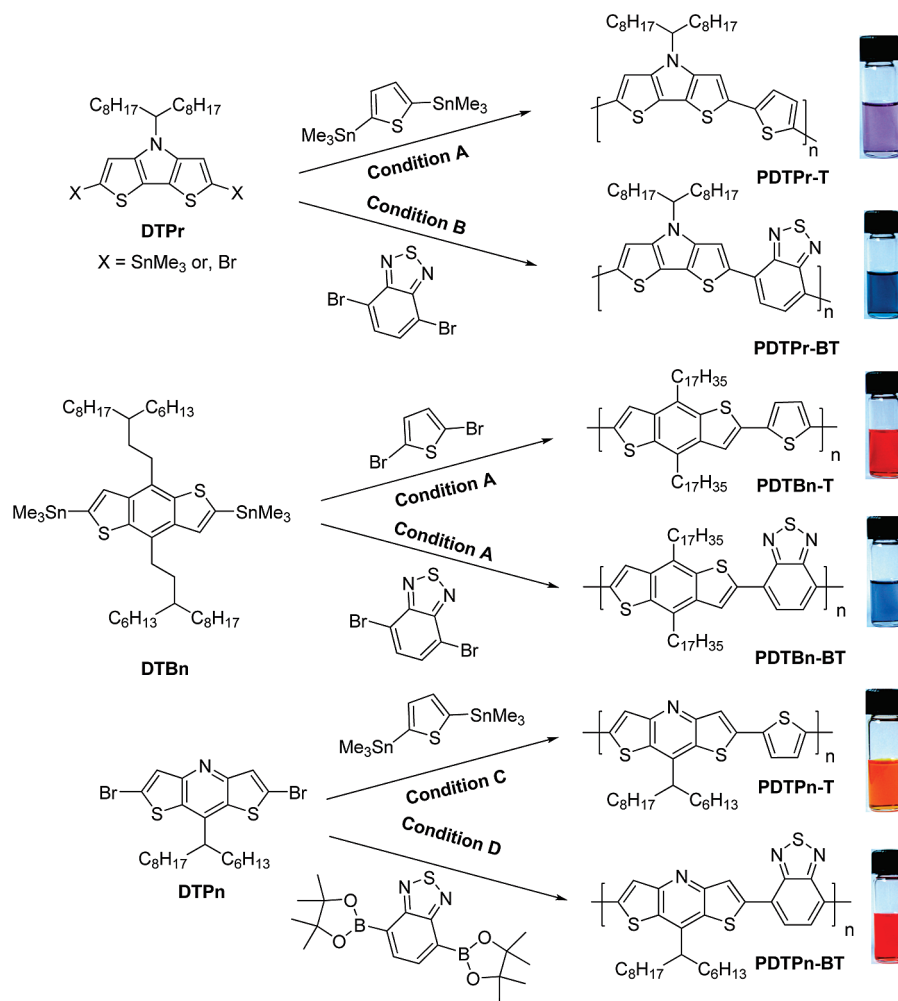


**Figure 2.** NMR results of lithiation study with deuterium labeling: (A) starting material, (B) product of *n*-BuLi lithiation and quench with  $\text{CD}_3\text{OD}$ , and (C) product of *tert*-BuLi lithiation and quench with  $\text{CD}_3\text{OD}$ .

mize the metalation procedure using *tert*-BuLi resulted in complete deprotonation with no traces of starting material; however, the deprotonation was not selective, resulting in a 57:43 mixture of  $\alpha$ : $\beta$  deprotonation. Therefore, a new synthetic route to prepare polymerizable 8-alkyldithienopyridines was required.

Because of these deficiencies with the literature preparation, a modified synthetic scheme (Scheme 1C) that introduced a bromine in the  $\alpha$ -position of the thiophene before condensation to form the pyridine ring was envisioned. The bromine was introduced in the first step by bromination of the commercially available thiophene-3-carboxylic acid.<sup>23</sup> The acid (**2**) was then subjected to a Curtius rearrangement to produce the Boc-protected amine (**3**) in good yield. The Boc protecting group stabilized the easily oxidized amine and was readily deprotected *in situ* in the subsequent acid-catalyzed condensation step. The aldehyde (**4**) was chosen to ensure the good solubility of the resulting polymers. The TFA-catalyzed condensation then afforded the final monomer (**5**) as a solid, which would aid in preparing high molecular weight polymers from typical condensation polymerizations where rigorous control of stoichiometry is required. This monomer (**5**) was then copolymerized with 2,5-bis(trimethyltin)thiophene or 2,1,3-benzothiadiazole-4,7-bis(boronic acid pinacol ester) to offer the desired polymers, **PDTPn-T** and **PDTPn-BT**.

### Scheme 2. Synthesis of Polymers via Palladium-Catalyzed Coupling Reactions<sup>a</sup>



**Conditions:** (A)  $\text{Pd}_2(\text{dba})_3$ ,  $\text{P}(\text{o-tol})_3$ , Toluene; (B)  $\text{Pd}(\text{PPh}_3)_4$ , Toluene; (C)  $\text{Pd}_2(\text{dba})_3$ ,  $\text{PPh}_3$ , Toluene; (D)  $\text{Pd}(\text{PPh}_3)_4$ ,  $\text{K}_2\text{CO}_3$ ,  $\text{H}_2\text{O}$ , Toluene

<sup>a</sup> Shown on the right are the representative solutions of each polymer.

The crude copolymers were washed extensively with methanol, followed by the Soxhlet extraction with methanol, and ethyl acetate successively to remove byproducts and oligomers. Finally, the polymers were Soxhlet extracted with hexanes or chloroform and recollected by precipitation into into methanol and dried under vacuum. The molecular structures of both polymers were confirmed by  $^1\text{H}$  NMR spectroscopy. The yields and molecular weights of polymers are listed in Table 1. The low yield of **PDTPPr-T** can be attributed to its low solubility, as large quantities of solid remained in the Soxhlet extraction thimble after chloroform extraction. The opposite problem explains the low polymer yield for **PDTBn-BT**, in that a large quantity of material was collected in the hexane fraction of the polymerization. However, this hexane fraction consisted of low molecular weight polymer, and only the high molecular weight chloroform fraction was used, decreasing the polymerization yield significantly. The molecular weights were determined by gel permeation chromatography (GPC) in THF or 1,2,4-trichlorobenzene by referring to polystyrene standards (Table 1). The molecular weights of **DTPn**-based polymers (**PDTPn-T** and **PDTPn-BT**) are noticeably low, which can be attributed to their lower solubility during the polymerization reaction.

**Optical and Electrochemical Properties.** This collection of structurally similar yet energetically diverse polymers allows for the interplay between the electron-donating ability of the donor monomer and the optical and electronic properties to be studied in detail. The optical and electrochemical properties of these polymers are shown in Figures 3 and 4, and extracted data are summarized in Table 2.

Interestingly, the HOMO energy level of the entire conjugated polymer is dominated primarily by the most electron-rich aromatic unit in the polymer, regardless of what other rings it is fused to. For example, nearly identical HOMO levels of  $-4.89$  and  $-4.94$  eV were observed in **PDTPPr-T** and **PDTPPr-BT**, respectively, because the most easily oxidized ring in these two polymers is the pyrrole ring. Therefore, the monomer **DTPPr** is polymerized with (**BT** or **T**) has little effect on the HOMO energy level, and this phenomena is common with other polymer systems.<sup>24</sup> However, when the pyrrole ring is substituted for a benzene or pyridine ring, a drastic reduction in the HOMO energy level is

observed. Since the newly substituted benzene or pyridine ring is no longer the most electron-rich ring in the system, the HOMO is relatively independent of which ring is substituted for the pyrrole ring. For example, nearly the same HOMO energy levels ( $-5.55$  eV vs  $-5.56$  eV) are measured for **PDTBn-BT** and **PDTPn-BT**. This is because the HOMO behavior is dominated by the two flanking thiophene rings. The same trend is apparent in the case of **PDTBn-T** and **PDTPn-T**, as the HOMO behavior is dominated by the copolymerized thiophene ring and causes the HOMO position to be roughly equal for both polymers despite their structural differences.

Despite the HOMO energy level depending greatly on the most electron-rich ring in the aromatic system, the optical band gap involves the entire polymeric system. Even though the HOMO energy level of the **DTPn** polymer series is little changed from the **DTBn** series, the band gaps of the **DTPn** series are significantly wider than these of the **DTBn** series. For example, the band gap of **PDTPn-BT** (2.1 eV) is noticeably larger than that of **PDTBn-BT** (1.8 eV) due to the electron-deficient pyridine, which diminishes the donor-acceptor interaction in the copolymer that gives the low band gap.

On the basis of electrochemical and optical considerations alone, **DTBn** is the most promising candidate for use in photovoltaic devices. The low measured HOMO energy levels predict high values of the  $V_{oc}$ , and the measured optical band gap remains low. Conversely, these results exhibit the **DTPn** and **DTPPr** units less favorably as possible successful candidates for use in photovoltaic devices. The band gaps of polymers made from the **DTPn** donor unit are significantly wider than the others in this study, while the HOMO levels are almost identical to the HOMO levels of the **DTBn** series. While polymers based upon **DTPPr** should have large theoretical maximum currents due to their lower band gaps, the HOMO levels of this series of polymers remain too high to yield devices with high efficiencies.

**Photovoltaic Properties.** These structurally similar, yet optically and electrochemically very different, polymers were tested in bulk heterojunction photovoltaic devices. Standard BHJ device configuration was used (ITO/PEDOT/polymer:PCBM/Ca/Al). A calibrated AM 1.5G light source (100 mW/cm<sup>2</sup>, 1 sun) was employed to simulate the irradiation from the sun. The blending ratio of polymer vs PCBM and the thickness of the active layer were varied to achieve the best device performance under semioptimized conditions (Table 3). Representative  $J-V$  curves of these polymers under 1 sun condition are displayed in Figure 5. In addition, the UV-vis and IPCE spectra of the **PDTBn-BT**/PCBM blend are displayed together (Figure 6) in order to reveal their correlation.

The **PDTBn** series immediately exhibits superior photovoltaic properties when compared to the rest of the polymers in this study. The theoretical predicted  $V_{oc}$  of 0.95 and 0.75 V for **PDTBn-BT** and **PDTBn-T**,<sup>25–27</sup> respectively, are close to

Table 1. Polymerization Results for Polymers

	yield [%]	$M_n$ [kg/mol]	$M_w$ [kg/mol]	PDI
<b>PDTPPr-T</b>	13	12.2 <sup>a</sup>	50.3 <sup>a</sup>	4.1
<b>PDTPPr-BT</b>	63	8.0 <sup>b</sup>	17.6 <sup>b</sup>	2.20
<b>PDTBn-T</b>	93	54.1 <sup>b</sup>	109.6 <sup>b</sup>	2.02
<b>PDTBn-BT</b>	8	69.9 <sup>b</sup>	150.7 <sup>b</sup>	2.15
<b>PDTPn-T</b>	90	4.3 <sup>a</sup>	10.7 <sup>a</sup>	2.47
<b>PDTPn-BT</b>	76	1.5 <sup>a</sup>	2.6 <sup>a</sup>	1.68

<sup>a</sup>Determined by GPC in 1,2,4-trichlorobenzene using polystyrene standard at 150 °C. <sup>b</sup>Determined by GPC in THF using polystyrene standards.

Table 2. Optical and Electrochemical Data of All Polymers

polymer	UV-vis absorption						cyclic voltammetry	
	CHCl <sub>3</sub> solution			film			$E_{onset}^{ox}$ (V)	$E_{onset}^{red}$ (V)
	$\lambda_{max}$ [nm]	$\lambda_{onset}$ [nm]	$E_g^a$ [eV]	$\lambda_{max}$ [nm]	$\lambda_{onset}$ [nm]	$E_g^a$ [eV]	HOMO [eV]	LUMO [eV]
<b>PDTPPr-T</b>	575	659	1.9	609	663	1.9	0.09/−4.89	−2.24/−2.56
<b>PDTPPr-BT</b>	697	837	1.5	727	875	1.4	0.14/−4.94	−1.73/−3.07
<b>PDTBn-T</b>	537	566	2.2	543	584	2.1	0.55/−5.35	−2.18/−2.62
<b>PDTBn-BT</b>	648	688	1.8	650	694	1.8	0.75/−5.55	−1.55/−3.25
<b>PDTPn-T</b>	465	535	2.3	465	534	2.3	0.63/−5.43	−1.83/−2.97
<b>PDTPn-BT</b>	508	580	2.1	540	579	2.1	0.76/−5.56	−1.47/−3.33

<sup>a</sup> Calculated from the intersection of the tangent on the low energetic edge of the absorption spectrum with the baseline.

the experimentally determined values of 0.77 and 0.88 V. Not surprisingly, the lower HOMO of the polymers (e.g., **PDTBn-BT**) yields relatively higher  $V_{oc}$  values. The moderately low band gaps in the **DTBn** series are sufficient to produce satisfactory short-circuit currents. Additionally, the symmetrical nature of the monomer combined with the alkyl chain branching being located on a carbon that is not adjacent to the polymer backbone should yield polymer films with higher crystallinity. Thus, despite a wider band gap, the high molecular weight and possible increased crystallinity of the blended film cause the short-circuit current of the **DTBn** series to be very close to that of the **DTPr** series of polymers.

As predicted, the low  $V_{oc}$  of the polymers in the **DTPr** series remains the limiting factor in their solar cell performance, with both cells recording  $V_{oc}$  values lower than 0.5 V. **PDTPr-BT**'s especially low band gap does lead to a 32% increase in the  $J_{sc}$  compared with that of **PDTBn-BT**; however, a significantly higher current must be obtained in order to offset its low  $V_{oc}$  (0.46 V) and fill factor (0.39). While these parameters can be improved by increases in molecular weight and further optimizing the polymer structure (modifying the alkyl chain length, varying the acceptor other than BT, etc.), the D-A polymers based on **DTPr** are intrinsically limited by their high-lying HOMO energy levels. Therefore, **DTPr** is not a particularly promising candidate for constructing new polymers as high efficiency photovoltaic materials. However, applications which require especially low band gaps (for example, infrared detectors) are still a possibility for this electron-rich donor monomer.

The **DTPn** series does not behave as expected in terms of  $V_{oc}$ . The experimentally determined values are significantly lower than the  $V_{oc}$  expected given the low HOMO levels of the polymers in this series. The poor performance of **PDTPn-BT** is likely due to its low molecular weight. 1.2 kg/mol represents a degree of polymerization of 2.25, and the effects of low molecular weight on all aspects of solar cell performance are well documented.<sup>28–31</sup> Additionally, the large branched alkyl chain adjacent to the polymer backbone in the **DTPn** (and **DTPr**) series could lead to amorphous films, which would reduce the efficiency of charge separation in the

BHJ device.<sup>32</sup> However, further optimization of the polymer structure was not warranted given the poor energetic and optical properties of this series of polymers.

The relatively low efficiencies of these polymer-based BHJ devices are mainly due to their low current, though low band gaps have been achieved in some of these polymers (e.g., **PDTPr-BT** and **PDTBn-BT**). In addition to a low band gap, a high hole mobility, comparable to the electron mobility of PCBM, is also required to achieve a high current. The hole mobility of these polymers in the BHJ blends was calculated via the space-charge limited current (SCLC) model by constructing hole-only devices with 40 nm of palladium (see Experimental Section for more details).<sup>33</sup> For comparison, “polymer only” devices were also fabricated to probe the mobility of polymers in the absence of PCBM.<sup>34</sup> The measured hole mobilities of these polymers in the absence of PCBM are generally much lower than the electron mobility of PCBM ( $\sim 10^{-4}$  cm<sup>2</sup>/(V s)) (Table 4), which explains the low efficiencies of these devices when compared with P3HT and other high-performance polymers. Additionally, the film morphology of these devices is not optimal. For example, AFM images of **PDTBn-T** based devices (see Supporting Information) reveal micrometer-sized phase

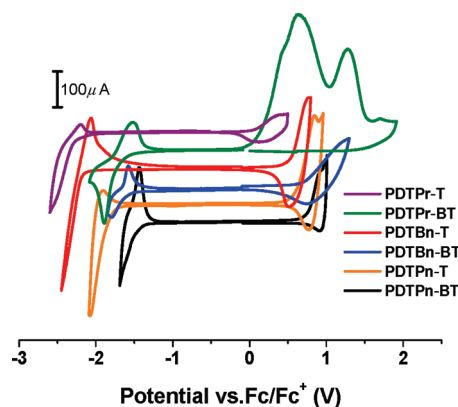


Figure 4. Cyclic voltammograms of all polymers.

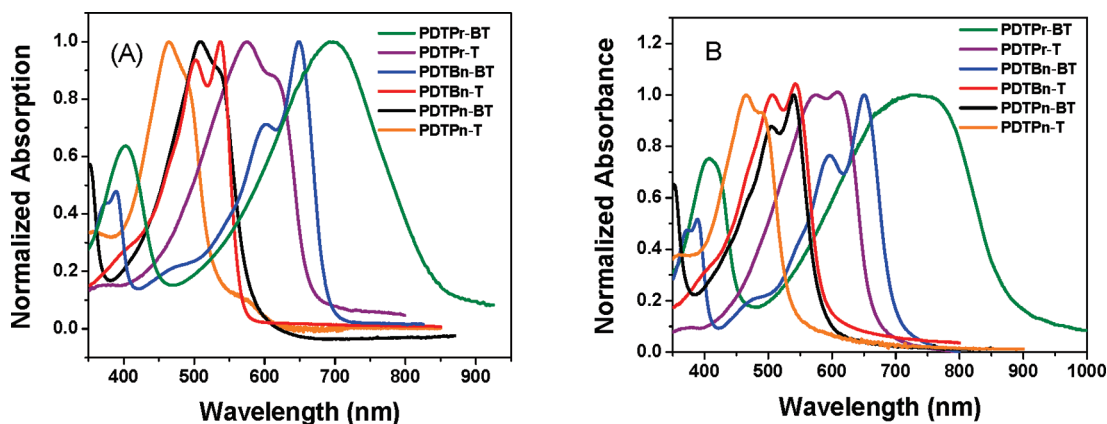
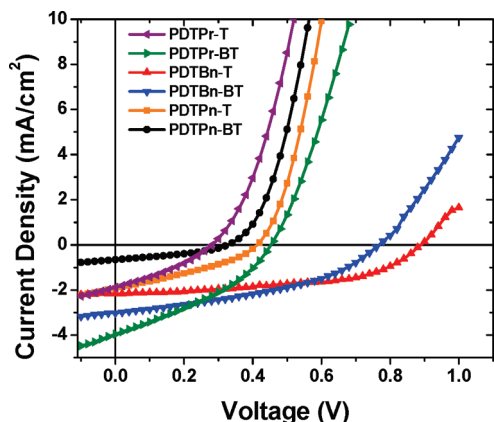


Figure 3. (A) Solution absorption of all polymers in chloroform. (B) Film absorptions.

Table 3. PV Performances of Polymers

polymer	polymer:PCBM	thickness (nm)	$V_{oc}$ (V)	$J_{sc}$ (mA/cm <sup>2</sup> )	FF	$\eta$ (%)	IPCE (%)	$R_s$ ( $\Omega$ )
PDTPr-T	1:1	50	0.29	1.89	0.32	0.18	0.58	117
PDTPr-BT	1:3	100	0.46	4.0	0.39	0.72	33.1	78
PDTBn-T	1:2	190	0.88	2.17	0.54	1.02	8.62	147
PDTBn-BT	1:1	155	0.77	3.02	0.41	0.94	16.1	80
PDTPn-T	1:3	50	0.41	1.93	0.34	0.27	10.1	48.7
PDTPn-BT	1:1	45	0.31	0.75	0.37	0.09	5.16	80



**Figure 5.** Characteristic  $I$ - $V$  curves of the optimized devices of all polymer-based BHJ solar cells under 1 sun condition.

**Table 4. Mobility**

polymer	thickness (nm)	mobility $\text{cm}^2/\text{V}\cdot\text{s}$	polymer:PCBM	thickness (nm)	mobility $\text{cm}^2/\text{V}\cdot\text{s}$
PDTPr-T	130	$1.11 \times 10^{-5}$	1:1	75	$8.17 \times 10^{-6}$
PDTPr-BT	120	$6.41 \times 10^{-5}$	1:3	75	$1.15 \times 10^{-5}$
PDTBn-T	80	$2.57 \times 10^{-5}$	1:2	65	$2.14 \times 10^{-6}$
PDTBn-BT	105	$2.75 \times 10^{-5}$	1:1	240	$3.88 \times 10^{-7}$
PDTPn-T	60	$5.98 \times 10^{-6}$	1:3	45	$3.55 \times 10^{-6}$
PDTPn-BT	100	$5.35 \times 10^{-6}$	1:1	45	$2.25 \times 10^{-6}$

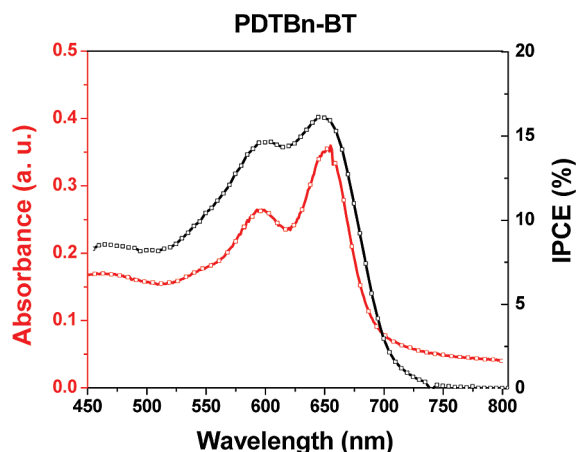


**Figure 6.** IPCE spectrum of BHJ photovoltaic device of ITO/PEDOT:PSS (45 nm)/PDTBn-BT:PCBM (1:1, w/w)/Ca (30 nm)/Al (100 nm) and the optical absorptions for the corresponding film of the blend.

segregation (even though PDTBn-T based devices exhibited the highest efficiency). Thus, these devices offer a preliminary look at the potential of these polymers, and employing additional optimization techniques beyond simple device thickness and ratio of polymer:PCBM could allow for an increase in device performance.

## Conclusion

We investigated a collection of six electrochemically and optically unique polymers based upon three donor monomers. All three donor monomers are structurally related, featuring the same flanking thiophenes, but incorporating different center aromatic units. DTBn-based polymers exhibited the most potential in photovoltaic applications due to its moderately low band gap and low HOMO energy level. The other polymers in this study either demonstrated high-lying HOMO energy levels (DTPr-based polymers) or unacceptably wide band gaps (DTPn-based polymers).

Two key structure/property trends have also emerged. The behavior of the HOMO energy level is dominated by the most electron-rich ring in the polymer backbone. Conversely, the optical band gap is a function of the electronic properties of the entire conjugated aromatic backbone. Electron-deficient pyridine diminishes the donor-acceptor interaction in the copolymer that gives the low band gap. This explains the 0.3 eV change in the band gap between DTBn-BT and DTPn-BT and the 0.3 eV change in band gap between DTBn-T and DTPr-T.

Lastly, the photovoltaic performance of DTBn polymer series is largely inhibited by the low hole mobility of the two polymer candidates. Future study will focus on improving the hole mobility and crystallinity of these polymers in order to improve their photovoltaic performance.

## Experimental Section

**General Methods.**  $^1\text{H}$  nuclear magnetic resonance (NMR) spectra were obtained at 400 or 300 MHz as solutions in  $\text{CDCl}_3$ .  $^{13}\text{C}$  NMR spectra were obtained at 100 MHz as solutions in  $\text{CDCl}_3$ . Chemical shifts are reported in parts per million (ppm,  $\delta$ ) and referenced from tetramethylsilane. Coupling constants are reported in hertz (Hz). Spectral splitting patterns are designated as s, singlet; d, doublet; t, triplet; m, multiplet; and br, broad. Melting points are uncorrected.

UV-vis absorption spectra were obtained by a Shimadzu UV-2401PC spectrophotometer. Fluorescence spectra were recorded on a Shimadzu RF-5301PC spectrofluorophotometer. For the measurements of thin films, the polymer was spin-coated at 600 rpm onto precleaned glass slides from 10 mg/mL polymer solution in *o*-dichlorobenzene and dried slowly in a Petri dish for 3 h.

Gel permeation chromatography (GPC) measurements were performed on two different machines, depending upon the solubility of the polymers in THF. For THF-soluble polymers, a Waters 2695 separations module apparatus with a differential refractive index detector (at UNC Chapel Hill) was used, employing tetrahydrofuran (THF) as the eluent. For THF nonsoluble polymers, a Polymer Laboratories PL-GPC 220 instrument (at University of Chicago) was used, using 1,2,4-trichlorobenzene as the eluent (stabilized with 125 ppm BHT) at 150 °C. The obtained molecular weight is relative to polystyrene standards.

Cyclic voltammetry measurements were carried out using a Bioanalytical Systems (BAS) Epsilon potentiostat equipped with a standard three-electrode configuration. Typically, a three-electrode cell equipped with a glassy carbon working electrode, a  $\text{Ag}/\text{AgNO}_3$  (0.01 M in anhydrous acetonitrile) reference electrode, and a Pt wire counter electrode was employed. The measurements were done in anhydrous acetonitrile with tetrabutylammonium hexafluorophosphate (0.1 M) as the supporting electrolyte under an argon atmosphere at a scan rate of 100 mV/s. Polymer films were drop-cast onto the glassy carbon working electrode from a 2.5 mg/mL chloroform solution and dried under house nitrogen stream prior to measurements. The potential of  $\text{Ag}/\text{AgNO}_3$  reference electrode was internally calibrated by using the ferrocene/ferrocenium redox couple ( $\text{Fc}/\text{Fc}^+$ ). The electrochemical onsets were determined at the position where the current starts to differ from the baseline. The highest occupied molecular orbital (HOMO) and lowest unoccupied molecular orbital (LUMO) energy levels were calculated from the onset oxidation potential ( $E_{\text{ox}}$ ) and onset reductive potential ( $E_{\text{red}}$ ), respectively, according to eqs 1 and 2.

$$\text{HOMO} = -(E_{\text{ox}} + 4.8) \text{ (eV)} \quad (1)$$

$$\text{LUMO} = -(E_{\text{red}} + 4.8) \text{ (eV)} \quad (2)$$

**Polymer Solar Cell Fabrication and Testing.** Glass substrates coated with patterned indium-doped tin oxide (ITO) were purchased from Thin Film Devices, Inc. The 150 nm sputtered

ITO pattern had a resistivity of 15  $\Omega/\square$ . Prior to use, the substrates were ultrasonicated for 10 min in acetone followed by deionized water and then 2-propanol. The substrates were dried under a stream of nitrogen and subjected to the treatment of UV-ozone over 20 min. A filtered dispersion of PEDOT:PSS in water (Baytron PH500) was then spun-cast onto clean ITO substrates at 4000 rpm for 60 s and then baked at 140 °C for 10 min to give a thin film with a thickness of 40 nm. A blend of polymer and PCBM (1:1, 1:2, or 1:3, w/w, depending upon the polymer; see Table 3) at 10 mg/mL (for polymer) was dissolved in dichlorobenzene (for PDTP-BT) or chlorobenzene (for other polymers) with heating at 60 °C for 6 h, filtered through a 0.45  $\mu\text{m}$  poly(tetrafluoroethylene) (PTFE) filter, and spun-cast between 800 and 1200 rpm for 60 s onto a PEDOT:PSS layer. The substrates were then dried at room temperature under  $\text{N}_2$  for 12 h. The devices were finished for measurement after thermal deposition of a 30 nm film of calcium and a 100 nm aluminum film as the cathode at a pressure of  $\sim 1 \times 10^{-6}$  mbar. There are eight devices per substrate, with an active area of 12  $\text{mm}^2$  per device. The thicknesses of films were recorded by a profilometer (Alpha-Step 200, Tencor Instruments). Device characterization was carried out under AM 1.5G irradiation with the intensity of 100  $\text{mW}/\text{cm}^2$  (Oriel 91160, 300 W) calibrated by a NREL certified standard silicon cell. Current vs potential ( $I$ - $V$ ) curves were recorded with a Keithley 2400 digital source meter. EQE were detected under monochromatic illumination (Oriel Cornerstone 260 1/4 m monochromator equipped with Oriel 70613NS QTH lamp), and the calibration of the incident light was performed with a monocrystalline silicon diode. All fabrication steps after adding the PEDOT:PSS layer onto ITO substrate, and characterizations were performed in gloveboxes under a nitrogen atmosphere. For mobility measurements, the hole-only devices in a configuration of ITO/PEDOT:PSS (45 nm)/polymer-PCBM/Pd (40 nm) were fabricated. The experimental dark current densities  $J$  of polymer:PCBM blends were measured when applied with voltage from 0 to 6 V. The applied voltage  $V$  was corrected from the built-in voltage  $V_{\text{bi}}$ , which was taken as a compensation voltage  $V_{\text{bi}} = V_{\text{oc}} + 0.05 V$  and the voltage drop  $V_{\text{rs}}$  across the indium tin oxide/poly(3,4-ethylene-dioxythiophene):poly(styrenesulfonic acid) (ITO/PEDOT:PSS) series resistance and contact resistance, which is found to be around 35  $\Omega$  from a reference device without the polymer layer. From the plots of  $J^{0.5}$  vs  $V$  (Supporting Information), hole mobilities of copolymers can be deduced from

$$J = \frac{9}{8} \epsilon_r \epsilon_0 \mu_h \frac{V^2}{L^3}$$

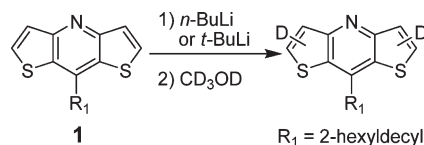
where  $\epsilon_0$  is the permittivity of free space,  $\epsilon_r$  is the dielectric constant of the polymer which is assumed to be around 3 for the conjugated polymers,  $\mu_h$  is the hole mobility,  $V$  is the voltage drop across the device, and  $L$  is the film thickness of active layer.

**Reagents.** All solvents are ACS grade unless otherwise noted. Anhydrous THF was obtained by distillation from sodium/benzophenone prior to use. Anhydrous methylene chloride was dried over magnesium sulfate and filtered directly into the reaction flask prior to use. Anhydrous toluene was used as received. Anhydrous *tert*-butanol was obtained by treatment with sodium metal and then distillation. 2-Bromothiophene-4-carboxylic acid,<sup>23</sup> 2,6-di(trimethyltin)-*N*-(1-octylonyl)dithieno[3,2-*b*:2',3'-*d*]pyrrole,<sup>18</sup> 2,5-bis(trimethyltin)thiophene,<sup>35</sup> 4,7-dibromo-2,1,3-benzothiadiazole,<sup>36</sup> and 2,1,3-benzothiadiazole-4,7-bis(boronic acid pinacol ester)<sup>37</sup> were prepared according to established literature procedures. 2,6-Bis(trimethyltin)-4,8-(3-hexylundecyl)benzo[1,2-*b*:4,5-*b'*]dithiophene<sup>6,20</sup> and *N*-(1-octylonyl)-2,6-dibromodithieno[3,2-*b*:2',3'-*d*]pyrrole<sup>38,39</sup> were prepared using procedures analogous to established literature procedures, and  $^1\text{H}$  and  $^{13}\text{C}$  NMR spectra for each monomer are shown in the Supporting Information. All other chemicals were purchased from commercial sources (Acros, Alfa Aesar, Aldrich, Fisher Scientific, Oakwood Chemical) and used without further purification.

***tert*-Butyl 5-Bromothiophen-3-ylcarbamate (3).** 2-Bromothiophene-4-carboxylic acid (11.584 g, 55.95 mmol) was combined with anhydrous toluene (225 mL) in a dry flask under argon. Triethylamine (11.8 mL, 83.93 mmol) was added to the slurry, which became homogeneous after addition. Diphenylphosphoryl azide (12.1 mL, 55.95 mmol) was then added at room temperature, and the reaction mixture was stirred for 2.5 h. The mixture was then heated to 80 °C and stirred for 1 h. Anhydrous *tert*-butanol (16.0 mL, 167.9 mmol) was then added, and the reaction mixture was stirred for 16 h at 80 °C. The mixture was then concentrated and purified by column chromatography using a 3:2 toluene:hexanes solution as the eluent. The fractions were concentrated, affording a beige powder of sufficient purity for the following steps. Yield: 11.807 g (76%). Analytical purity was obtained by recrystallization from cyclohexanes (refluxed, then cooled to 4 °C), yielding colorless prisms which were stable in atmosphere for over a week. Colorless crystalline solid; mp 88–91 °C.  $^1\text{H}$  NMR ( $\text{CDCl}_3$ , 300 MHz,  $\delta$ ): 7.04 (br s, 1H), 6.94 (br s, 1H), 6.61 (br s, 1H), 1.50 (s, 9H).  $^{13}\text{C}$  NMR ( $\text{CDCl}_3$ , 100 MHz,  $\delta$ ): 152.5, 135.8, 123.7, 111.7, 108.7, 80.9, 28.2. ESI-TOF MS:  $[\text{M} + \text{Na}]^+ = 299.9667$  (calcd  $[\text{M} + \text{Na}]^+ = 299.9670$ ).

**2,6-Dibromo-8-(1-hexylonyl)dithieno[3,2-*b*:2',3'-*e*]pyridine (5).** 3 (2.039 g, 7.33 mmol) and 2-hexyldecanal (881 mg, 3.67 mmol) were dissolved in methylene chloride (40 mL). Trifluoroacetic acid (1.8 mL) was slowly added over 3 min, and the resulting mixture was heated to reflux. After 18 h, the reaction mixture was partitioned between  $\text{CH}_2\text{Cl}_2$  and ice cold 10% NaOH solution and separated, and the organic layer was dried over  $\text{Na}_2\text{SO}_4$ . The mixture was then purified by column chromatography eluting with a 7:1 mixture of hexanes:ethyl acetate. The resulting yellow oil was then concentrated under vacuum (0.5 mmHg) for 24 h, resulting in a pale brown solid. Yield: 615 mg (30%). Crystalline brown solid; mp 60–61 °C.  $^1\text{H}$  NMR ( $\text{CDCl}_3$ , 300 MHz,  $\delta$ ): 7.57 (s, 2H), 2.99 (m, 1H), 2.01 (m, 2H), 1.84 (m, 2H), 1.16 (m, 20H), 0.86 (m, 6H).  $^{13}\text{C}$  NMR ( $\text{CDCl}_3$ , 100 MHz,  $\delta$ ): 154.98, 141.66, 127.66, 120.93, 47.02, 33.51, 33.47, 31.72, 31.49, 29.48, 29.19, 29.10, 27.79, 22.55, 22.48, 13.99, 13.91. ESI-TOF MS  $[\text{M} + \text{H}]^+ = 558.0506$  (calcd  $[\text{M} + \text{H}]^+ = 558.0499$ ).

**2-Hexyldecanal (4).** Dimethyl sulfoxide (10.2 mL, 143.6 mmol) was dissolved in anhydrous methylene chloride (350 mL) and chilled to  $-78$  °C under argon. Oxalyl chloride (6.48 mL, 75.6 mmol) was then slowly added dropwise, while maintaining the temperature at  $-78$  °C. The mixture was stirred for 30 min, and then 2-hexyldecan-1-ol (20.9 mL, 71.99 mmol) was added dropwise at  $-78$  °C. The mixture was stirred for 35 min carefully maintaining  $-78$  °C. TEA (30 mL, 215 mmol) was added, and a thick white precipitate formed. The mixture was stirred for 10 min at  $-78$  °C and then allowed to warm to room temperature. The mixture was poured into 1 M HCl and extracted with methylene chloride. The organic layer was then washed repeatedly with distilled water and dried over  $\text{MgSO}_4$ . The mixture was then filtered, concentrated, and filtered through a short plug of silica gel. The silica gel was washed with hexanes, and the filtrate was concentrated and distilled under reduce pressure. The desired aldehyde was obtained at a distillate temperature of 105 °C at 0.6 mmHg. Yield: 12.087 g (70%). Colorless oil.  $^1\text{H}$  NMR ( $\text{CDCl}_3$ , 300 MHz,  $\delta$ ): 9.55 (d,  $J = 3.3$  Hz, 1H), 2.21 (m, 1H), 1.60 (m, 2H), 1.45 (m, 2H), 1.27 (m, 20H), 0.88 (t,  $J = 6.6$  Hz, 6H).  $^{13}\text{C}$  NMR ( $\text{CDCl}_3$ , 100 MHz,  $\delta$ ): 205.45, 51.94, 31.80, 31.59, 29.66, 29.35, 29.32, 29.18, 28.88, 27.03, 26.99, 22.59, 22.52, 14.00, 13.95.



**Deuterium Lithiation Experiments.** The following lithiation conditions are reproduced from ref 21. **1** (151 mg, 0.363 mmol)

was dissolved in 1.5 mL of anhydrous THF in a dry flask. The solution was cooled to  $-78\text{ }^{\circ}\text{C}$ , and a 2.5 M solution of *n*-BuLi in hexanes (0.35 mL, 0.87 mmol) was added dropwise. The solution was stirred at  $-78\text{ }^{\circ}\text{C}$  for 1 h and then at  $0\text{ }^{\circ}\text{C}$  for 5 h. The solution was then cooled back down to  $-78\text{ }^{\circ}\text{C}$ , and methanol- $d_4$  (0.5 mL) was added in one portion. The solution was stirred at  $-78\text{ }^{\circ}\text{C}$  for 5 min and then warmed to room temperature. The reaction mixture was then filtered through a silica plug (250 mg), and the plug was washed with 1 mL of  $\text{CH}_2\text{Cl}_2$ . The resulting filtrate was then concentrated, and the residue was analyzed by NMR. The procedure was repeated using 2.05 equiv of *t*-BuLi at  $-78\text{ }^{\circ}\text{C}$  for 1 h and then quenching with methanol- $d_4$ .

**Representative Stille Coupling Polymerization Procedure.** 2,6-Bis(trimethyltin)-4,8-(3-hexylundecyl)benzo[1,2-*b*:4,5-*b'*]dithiophene (498 mg, 0.502 mmol), 4,7-dibromo-2,1,3-benzothiadiazole (147 mg, 0.502 mmol), tri(*o*-tolyl)phosphine (18 mg, 0.06 mmol), and 25 mL of anhydrous toluene were combined and purged with argon for 20 min. Then tris(dibenzylideneacetone)dipalladium(0) (7 mg,  $7.53 \times 10^{-3}$  mmol) was added under a stream of argon, and the reaction mixture was purged for an additional 15 min. The mixture was then heated to reflux and stirred for 72 h. The reaction mixture was then precipitated into methanol and filtered into an extraction thimble. The polymer solids were then Soxhlet extracted with methanol, ethyl acetate, hexanes, and chloroform. The chloroform extracts were then concentrated and precipitated into methanol. The resulting solids were filtered and washed with methanol, and residual solvent was removed under vacuum at 0.5 mmHg affording polymer PDTBn-BT as a blue-black powder. Yield: 32 mg (8%).

**Acknowledgment.** This work was supported by the University of North Carolina at Chapel Hill, the National Science Foundation STC Program at UNC Chapel Hill (CHE-9876674), a DuPont Science and Engineering Grant, a DuPont Young Professor Award, and the Office of Naval Research (Grant N000140911016). S.C.P. gratefully acknowledges Applied Materials for a graduate fellowship. We acknowledge Mr. Huaxing Zhou for CV measurements. We thank Prof. Richard Jordan and Mr. Zhongliang Shen of the University of Chicago for GPC measurements.

**Supporting Information Available:**  $^1\text{H}$  and  $^{13}\text{C}$  spectra of molecules;  $J^{0.5}$  vs  $V$  plots of mobility measurement of all polymers. This material is available free of charge via the Internet at <http://pubs.acs.org>.

## References and Notes

- Thompson, B. C.; Fréchet, J. M. J. *Angew. Chem., Int. Ed.* **2008**, *47*, 58.
- Bundgaard, E.; Krebs, F. C. *Sol. Energy Mater. Sol. Cells* **2007**, *91*, 954.
- Kroon, R.; Lenes, M.; Hummelen, J. C.; Blom, P. W. M.; de Boer, B. *Polym. Rev.* **2008**, *48*, 531.
- Dennler, G.; Scharber, M. C.; Brabec, C. J. *Adv. Mater.* **2009**, *21*, 1323.
- Park, S. H.; Roy, A.; Beaupre, S.; Cho, S.; Coates, N.; Moon, J. S.; Moses, D.; Leclerc, M.; Lee, K.; Heeger, A. J. *Nat. Photonics* **2009**, *3*, 297.
- Liang, Y.; Feng, D.; Wu, Y.; Tsai, S.-T.; Li, G.; Ray, C.; Yu, L. *J. Am. Chem. Soc.* **2009**, *131*, 7792.
- Peet, J.; Kim, J. Y.; Coates, N. E.; Ma, W. L.; Moses, D.; Heeger, A. J.; Bazan, G. C. *Nat. Mater.* **2007**, *6*, 497.
- Chen, C.-P.; Chan, S.-H.; Chao, T.-C.; Ting, C.; Ko, B.-T. *J. Am. Chem. Soc.* **2008**, *130*, 12828.
- Hou, J.; Chen, H.-Y.; Zhang, S.; Li, G.; Yang, Y. *J. Am. Chem. Soc.* **2008**, *130*, 16144.
- Wang, E.; Wang, L.; Lan, L.; Luo, C.; Zhuang, W.; Peng, J.; Cao, Y. *Appl. Phys. Lett.* **2008**, *92*, 033307.
- Wienk, M. M.; Turbiez, M.; Gilot, J.; Janssen, R. A. J. *Adv. Mater.* **2008**, *20*, 2556.
- Huang, F.; Chen, K.-S.; Yip, H.-L.; Hau, S. K.; Acton, O.; Zhang, Y.; Luo, J.; Jen, A. K. Y. *J. Am. Chem. Soc.* **2009**, *131*, 13886.
- Huo, L.; Hou, J.; Chen, H.-Y.; Zhang, S.; Jiang, Y.; Chen, T. L.; Yang, Y. *Macromolecules* **2009**, *42*, 6564.
- Liang, Y.; Wu, Y.; Feng, D.; Tsai, S.-T.; Son, H.-J.; Li, G.; Yu, L. *J. Am. Chem. Soc.* **2009**, *131*, 56.
- Xiao, S. Q.; Zhou, H. X.; You, W. *Macromolecules* **2008**, *41*, 5688.
- Xiao, S.; Stuart, A. C.; Liu, S.; You, W. *ACS Appl. Mater. Interfaces* **2009**, *1*, 1613.
- Westenhoff, S.; Howard, I. A.; Hodgkiss, J. M.; Kirov, K. R.; Bronstein, H. A.; Williams, C. K.; Greenham, N. C.; Friend, R. H. *J. Am. Chem. Soc.* **2008**, *130*, 13653.
- Koeckelberghs, G.; De Cremer, L.; Persoons, A.; Verbiest, T. *Macromolecules* **2007**, *40*, 4173.
- Radke, K. R.; Ogawa, K.; Rasmussen, S. C. *Org. Lett.* **2005**, *7*, 5253.
- Pan, H.; Li, Y.; Wu, Y.; Liu, P.; Ong, B. S.; Zhu, S.; Xu, G. *Chem. Mater.* **2006**, *18*, 3237.
- Sonar, P.; Zhang, J.; Grimsdale, A. C.; Mullen, K.; Surin, M.; Lazzaroni, R.; Leclere, P.; Tierney, S.; Heeney, M.; McCulloch, I. *Macromolecules* **2004**, *37*, 709.
- Heeney, M.; Tierney, S.; Thompson, M.; Giles, M.; Farrant, L.; Shkunov, M.; Sparrowe, D.; McCulloch, I. EP 1279689 A2, **2003**.
- Campaigne, E.; Bourgeois, R. C. *J. Am. Chem. Soc.* **1954**, *76*, 2445.
- Blouin, N.; Michaud, A.; Gendron, D.; Wakim, S.; Blair, E.; Neagu-Plesu, R.; Belletete, M.; Durocher, G.; Tao, Y.; Leclerc, M. *J. Am. Chem. Soc.* **2008**, *130*, 732.
- Brabec, C. J.; Cravino, A.; Meissner, D.; Sariciftci, N. S.; Fromherz, T.; Rispens, M. T.; Sanchez, L.; Hummelen, J. C. *Adv. Funct. Mater.* **2001**, *11*, 374.
- Gadisa, A.; Svensson, M.; Andersson, M. R.; Inganäs, O. *Appl. Phys. Lett.* **2004**, *84*, 1609.
- Mihailetchi, V. D.; Blom, P. W. M.; Hummelen, J. C.; Rispens, M. T. *J. Appl. Phys.* **2003**, *94*, 6849.
- Schilinsky, P.; Asawapirom, U.; Scherf, U.; Biele, M.; Brabec, C. J. *Chem. Mater.* **2005**, *17*, 2175.
- Ma, W.; Kim, J. Y.; Lee, K.; Heeger, A. J. *Macromol. Rapid Commun.* **2007**, *28*, 1776.
- Ballantyne, A. M.; Chen, L.; Dane, J.; Hammant, T.; Braun, F. M.; Heeney, M.; Duffy, W.; McCulloch, I.; Bradley, D. D. C.; Nelson, J. *Adv. Funct. Mater.* **2008**, *18*, 2373.
- Coffin, R. C.; Peet, J.; Rogers, J.; Bazan, G. C. *Nat. Chem.* **2009**, *1*, 657.
- Ohkita, H.; Cook, S.; Astuti, Y.; Duffy, W.; Tierney, S.; Zhang, W.; Heeney, M.; McCulloch, I.; Nelson, J.; Bradley, D. D. C.; Durrant, J. R. *J. Am. Chem. Soc.* **2008**, *130*, 3030.
- Mihailetchi, V. D.; Xie, H. X.; de Boer, B.; Koster, L. J. A.; Blom, P. W. M. *Adv. Funct. Mater.* **2006**, *16*, 699.
- Goh, C.; Kline, R. J.; McGehee, M. D.; Kadnikova, E. N.; Fréchet, J. M. J. *Appl. Phys. Lett.* **2005**, *86*, 122110.
- Furuta, P.; Fréchet, J. M. J. *J. Am. Chem. Soc.* **2003**, *125*, 13173.
- Liu, B.; Bazan, G. C. *Nat. Protoc.* **2006**, *1*, 1698.
- Zhang, M.; Tsao, H. N.; Pisula, W.; Yang, C.; Mishra, A. K.; Müllen, K. *J. Am. Chem. Soc.* **2007**, *129*, 3472.
- Odom, S. A.; Lancaster, K.; Beverina, L.; Lefler, K. M.; Thompson, N. J.; Coropceanu, V.; Brédas, J.-L.; Marder, S. R.; Barlow, S. *Chem. Eur. J.* **2007**, *13*, 9637.
- Lehmann, L. U. US 20080262183 A1, **2008**.